Water Sorption, Proton Conduction, and Methanol Permeation Properties of Sulfonated Polyimide Membranes Cross-Linked with *N*,*N*-Bis(2-hydroxyethyl)-2-aminoethanesulfonic Acid (BES)

Chang Hyun Lee,[†] Ho Bum Park,[†,‡] Youn Suk Chung,[†] Young Moo Lee,*[,†] and Benny D. Freeman[‡]

School of Chemical Engineering, Hanyang University, Seoul 133-791, South Korea, and Department of Chemical Engineering, University of Texas at Austin, Burnet Road 10100, Austin, Texas 78758

Received October 14, 2005; Revised Manuscript Received November 17, 2005

ABSTRACT: Sulfonated polyimide (SPI) membranes consisting of 1,4,5,8-naphthalenetetracarboxylic dianhydride (NTDA), 3,5-diaminobenzoic acid (DBA), and 4,4′-diaminodiphenyl ether 2,2′-disulfonic acid (SODA) were synthesized over a wide range of DBA/SODA molar compositions. A sulfonic acid-containing cross-linking agent, *N*,*N*-bis(2-hydroxyethyl)-2-aminoethanesulfonic acid (BES), was subsequently used to induce cross-linking between sulfonated polyimide chains via a thermally activated reaction. Efforts to prevent excessive water swelling due to the high degree of sulfonation and to avoid undesirable molecular transport by cross-linking typically resulted in a reduction of ion conductivity due to the blockage of a hydrophilic channel or loss of the water pocket after cross-linking. To solve this problem, a sulfonic acid-containing compound was used as both a cross-linking agent and a proton carrier. One of the main goals of this study was to compensate for the probable loss of ion conductivity due to cross-linking by using a cross-linker that included a fixed charge group. As expected, the BES-cross-linked SPI membranes showed excellent proton conductivity (i.e., $\sigma = 0.1$ S cm^{-1} at 90 °C and relative humidity (RH) of 90%) and low methanol permeability (i.e., $P = 1.6 \times 10^{-7}$ cm^2 s^{-1}). Proton conductivity increased and methanol permeability decreased with BES content, which is completely contrary to typical behavior as both properties are normally reduced by further cross-linking. In addition, the effect of cross-linking without a fixed charged group (-SO_3H) on the transport and permeation properties was compared with that of BES in cross-linked SPI membranes.

Introduction

Perfluorosulfonic acid ionomers such as Nafion membranes brought about a major breakthrough in polymer electrolyte membrane fuel cells (PEMFC). These membranes provide excellent chemical stability and high proton conductivity. The high proton conductivity is due to the high electronegativity of the fluorine atoms bonded to the same carbon atoms as the sulfonic acid group. That is, the high electronegativity makes the -SO_3H a superacid. Actually, the main reason that many sulfonated aromatic polymer membranes show low proton conductivity despite a high sulfonation level is because the acidity of the sulfonic groups attached to the phenylene group is lower than that of the sulfonic groups in the Nafion membranes.[1] One of the major remaining drawbacks of Nafion membranes is their high cost. Additionally, the reduction of the proton conductivity at elevated temperature and the high methanol crossover should be improved in Nafion membranes.

Currently, numerous sulfonated aromatic polymer membranes (partial-perfluorinated[2−5] or nonperfluorinated[6−16]) have been synthesized and tested for fuel cell applications. In general, they are synthesized from the post-sulfonation of a parent polymer[6−10] or monomer sulfonation-subsequent polymerization.[11−16] These sulfonated aromatic polymer membranes require a high sulfonation level to achieve sufficient proton conductivity, due to the low acidity of the sulfonic groups in the aromatic rings. Unfortunately, such a high sulfonation level makes them excessively water-swollen or soluble in water. Therefore, highly sulfonated polymer membranes lose their mechanical properties and become unavailable in applications.

Cross-linking could be a simple and powerful solution to control such indispensable properties including high proton conductivity, excellent mechanical properties, and good dimensional stability. So far, there have been several studies on the cross-linking of sulfonated polymer membranes including the cross-linking of sulfonated poly(ether ether ketone) (PEEK) via a thermally activated reaction of polyatomic alcohols and sulfonic acid groups,[17,18] the UV-assisted photo-cross-linking of sulfonated polyphosphazene (PPh),[19−21] the chemical cross-linking of poly(vinyl alcohol) and sulfosuccinic acid,[14,22] and the ionic cross-linking of acid−base blend membranes.[23,24] For the most part, the cross-linking resulted in a significant improvement of the chemical and mechanical stability, but the proton conductivity decreased with cross-linking.

In our previous study,[25] cross-linked sulfonated polyimides were prepared through the cross-linking of various diols with polymer segments containing carboxylic acid groups. Here, the chain length of the flexible cross-linkers in rigid sulfonated polyimide structures significantly affected the water sorption, proton conduction, and also methanol permeability. Above a certain chain length, the cross-linking significantly increased proton conductivity over that of the corresponding non-cross-linked sulfonated polyimide membranes, and also decreased the methanol permeability. In addition, despite ester bonding, the introduction of diol cross-linkers provided the resultant membranes with improved hydrolytic and oxidative stability.

In the present study, a cross-linker containing sulfonic acid groups was considered to determine the effect of a fixed charged group in cross-linking chains on water sorption, proton conduction, and methanol transport. Here, *N*,*N*-bis(2-hydroxylethyl)-

* Corresponding author. Telephone: +82-2-2220-0525. Fax: +82-2-2291-5982. E-mail: ymlee@hanyang.ac.kr.
[†] Hanyang University.
[‡] University of Texas at Austin.

10.1021/ma052226y CCC: $33.50
Published on Web 12/21/2005

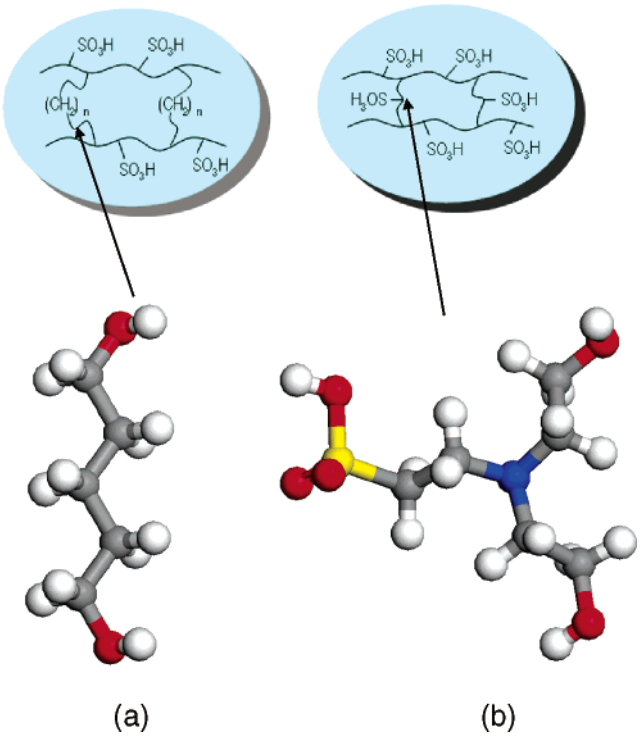

Figure 1. Schematic diagram of cross-linked sulfonated polyimides with (a) PtG cross-linker and (b) BES cross-linker.

2-aminoethanesulfonic acid (BES) was employed as a sulfonic acid-containing cross-linker. BES was chosen because the chain length of BES was comparable with the 1,5-pentanediol (PtG)-cross-linker used previously. We expected that the incorporation of a cross-linker containing a sulfonic acid group in the sulfonated polyimide membranes would help the membranes to have improved proton conductivity, mechanical properties, and also reduced methanol permeability. The goal of this study is to reveal the structure−property relationships between cross-linked sulfonated membranes and types of cross-linkers, in comparison with the non-cross-linked and cross-linked system without sulfonic acid groups. For comparison, a PtG-cross-linked sulfonated polyimide membrane was fabricated. The PtG and BES cross-linkers are comparable with each other because they have a similar chain length, and also the ionic radius of the carbon atoms in PtG (29 pm, four-cooridnate, tetrahedral) is similar to that of the nitrogen atoms in BES (30 pm, six-coordinate, octahedral), as shown in Figure 1.[26]

Experimental Section

Materials. 1,4,5,8-Naphthalenetetracarboxylic dianhydride (NTDA), 3,5-diaminobenzoic acid (DBA), 4,4′-diaminodiphenyl ether (ODA), and *N*,*N*-bis(2-hydroxyethyl)-2-aminoethanesulfonic acid (BES) were purchased from Tokyo Kasei Co. (Tokyo, Japan) and used as received. Concentrated sulfuric acid (95%, Aldrich, WI) and fuming sulfuric acid, SO_3 (30%, Aldrich, WI), were used in the sulfonation of ODA and resulted in 4,4′-diaminodiphenyl ether 2,2′-disulfonic acid (SODA).[27] *m*-Cresol (99%, Aldrich, MI) was used as a solvent. Benzoic acid (BAc) and triethylamine (Et_3N; Aldrich, WI) were used as a catalyst and a liberator of the protonated groups, respectively. Toluene as an azotropic compound and 1,5-pentanediol (PtG) as a cross-linker were purchased from Aldrich (WI).

Synthesis of Sulfonated Copolyimides (SPI-Y). SPI-III was synthesized by a solution-thermal imidization method, using SODA (1.6 mmol), DBA (2.4 mmol), and NTDA (4.0 mmol) as previously reported.[25] In the nomenclature of SPI-Y, the Roman numerals (I, II, and III) indicate the mole ratios (4/6, 5/5, and 6/4) of DBA to SODA.

Synthesis of Cross-Linked Sulfonated Polyimides (XSPI-Y). Cross-linking with BES and PtG was carried out using 15 wt % SPI-Y solution in *m*-cresol. BES or PtG was added into the SPI-Y solutions. Then, the mixtures were stirred at 110 °C for 2 h and at 160 °C for 8 h. After the solution temperature cooled again to 110 °C, additional *m*-cresol was added to make dilute XSPI-Y solutions. The solutions were poured into cold acetone, and the resultant precipitates were filtered off, washed several times with cold acetone, and dried in a vacuum oven at 110 °C for at least 2 days. For BES-cross-linked SPI membranes, the mole percent (*n*) of BES added into the SPI solutions was varied from 10 to 64 mol %, considering possible reaction sites (i.e., sulfonic acid groups in SODA + BES and carboxylic acid groups in DBA + BES) in order to determine the optimum amount of the cross-linker.

Membrane Preparation. All triethylammonium (Et_3N) salt-formed membranes were prepared using a solution-casting and evaporation method. The polymer solution concentration was 10 wt %. The cast membranes were dried at 80 °C for 2 h and then at 180 °C in a vacuum oven for 10 h for full imidization and thermal activation of the cross-linking reaction. Each membrane on the glass plate was soaked in methanol at room temperature and then peeled off from the glass plate by immersing them in deionized water. For conversion into the protonated form, the membranes were immersed in a 1 M HCl solution overnight. After acid treatment, the membranes were washed several times with deionized water and dried in a vacuum oven at 160 °C. Membrane thicknesses were in the range of 40−50 μm.

Membrane Characterization. Spectroscopic measurements of the SPI membranes were performed using a Fourier transform infrared spectrometer (FT-IR, Nicolet Magna IR 760 spectra ESP, WI) in the range of 400−2000 cm^{-1} and a ^1H and ^{13}C nuclear magnetic resonance (NMR, Varian model NMR 1000, CA) spectrometer. The solubility of the salt form polymers was examined to evaluate the apparent degree of cross-linking after vigorous stirring in various polar aprotic solvents such as dimethyl sulfoxide (DMSO), dimethylformamide (DMF), dimethyl acetate (DMAc), 1-methyl-2-pyrrolidinone (NMP), and *m*-cresol at room temperature for 3 days. The amount of insoluble residuals in a given solvent was compared with each other. The ion exchange capacity (IEC, mequiv g^{-1}) was measured using a classical titration method (ASTM D2187) with 0.01 M NaOH (titrant) and phenolphthalein (titration indicator) and also by elemental analysis (EA, Model EA 1108, Carlo Erba Instrument, Milan, Italy). The water uptake was measured by immersing the membrane coupons into deionized water at 30 °C for at least 1 day, then removing the samples and blotting the membrane surface to remove any excess water, and finally, promptly weighing them on a microbalance. The water uptake was expressed as follows:

$$W = \frac{(W_w - W_d)}{W_d} \quad (1)$$

where, W_d and W_w are the mass of the dry sample and the mass of the water-swollen sample, respectively. The amount of free water in fully hydrated SPI membranes was determined by differential scanning calorimetry (DSC, DSC 2010 thermal analyzer, TA Instruments, DE) measurements. A wet membrane sample was hermetically sealed in a sample pan. A differential scanning calorimetry (DSC) module was purged with nitrogen gas and quenched down to −50 °C with liquid nitrogen and then heated to +50 °C. The thermal degradation behavior of the SPI membranes was measured using a TGA 2050 thermogravimetric analyzer (TA Instruments, DE) at a heating rate of 10 °C min^{-1} from room temperature to 550 °C. The average *d*-spacing value (Å) was obtained from a wide-angle X-ray diffraction (WAXD) pattern using a Rigaku Denki Model RAD-C diffractometer (Tokyo, Japan). The X-ray generator was run at 40 kV and 100 mA. The proton conductivity of each membrane coupon (size: 1 cm × 4 cm) was measured using an electrode system connected with an impedance/gain-phase analyzer (Solatron 1260) and an electrochemical inter-

face (Solatron 1287, Farnborough Hampshire, ONR, U.K.). Four-point-probe alternating current (ac) impedance spectroscopy was used to eliminate the inductive impedance caused by the electric conductive leads and potentiometer and also to measure more accurate membrane impedance. Further concrete information can be found in our previous work.[28] The proton conductivity was obtained using the following equation:

$$\sigma = \frac{l}{RS} \tag{2}$$

where σ is the proton conductivity in S cm^{-1}, R is the ohmic resistance of the membrane, l is the distance between reference electrodes, and S is the cross-sectional area of the membrane. The impedance measurement was carried out in an automatically thermo- and hygrocontrolled chamber that was electrically shielded to ensure a stable measurement without any noise. In addition, the temperature dependence upon the proton conductivity of the SPI membranes was obtained from the Arrhenius equation as follows:

$$\ln \sigma = -\frac{E_a}{RT} \tag{3}$$

where E_a is the activation energy in kJ mol^{-1}, R is the universal gas constant (8.314 J mol^{-1} K^{-1}), and T is the absolute temperature in K. Methanol permeability (P, cm^2 s^{-1}) was measured using a two-chamber diffusion cell. One 60 mL chamber contained a 10 M methanol solution, and the other 60 mL chamber was filled with deionized water. A membrane was placed between the two chambers, and the methanol concentration was periodically detected by a GC-14B gas chromatograph (Shimadtzu, Tokyo, Japan) equipped with a thermal conductivity detector (TCD). P was obtained from the following equation:

$$P = \frac{(V_B L)}{(C_A A)} \frac{C_B(t)}{t} f \tag{4}$$

where V_0 is the initial volume of deionized water, L is the membrane thickness, A is the membrane area, C_A is the initial concentration, $C_B(t)$ is methanol concentration at time t, and f is the conversion factor by GC calibration. Hydrolytic stability was also examined in deionized water at 80 °C and in the 30 wt % H_2O_2 and 0.1 wt % ferrous ammonium sulfate solutions, respectively.

Results and Discussion

Characterization of SPI Membranes. A previously synthesized sulfonated diamine (SODA) was successfully introduced into a hydrolytic stable naphthalenic polyimide structure to avoid severe chemical degradation and chain scission by post-sulfonation. When sulfonated five-membered phthalic polyimide membranes are used for proton exchange membranes in fuel cells, they degrade quickly and become brittle and fragile. This is because under strong acid conditions, the hydrolysis of the phthalimide structure results in chain scission.[29] Fortunately, naphthalenic imide structures do not quickly degrade and are much more stable to hydrolysis.[29,30]

There have already been reports in the literature regarding proton transport behavior through sulfonated polyimide membranes derived from a naphthalenic dianhydride and a sulfonated diamine.[27,31−34] These sulfonated polyimides showed excellent proton conductivities as compared to other sulfonated polymers and exhibited better dimensional stability even at a high water-swollen state. Mostly, sulfonated six-membered ring polyimide membranes were synthesized in the copolymer form to control the hydrophilic (sulfonated diamine + dianhydride) and hydrophobic (nonsulfonated diamine + dianhydride) nature. The original idea for this combination arose from an analogue of the Nafion structure which consists of hydrophilic and hydrophobic domains. However, the addition of hydrophobic domains leads to a large reduction in the proton conductivity, and it is difficult to find the appropriate chemical composition at which the maximum proton conductivity and excellent mechanical properties are obtained.

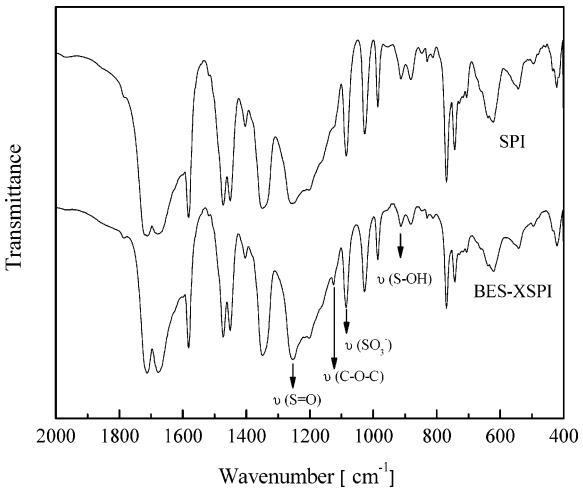

Figure 2. FT-IR spectrum of BES−XSPI-III compared with SPI-III.

In this study, various sulfonated polyimides based upon the NTDA−SDA−DBA structure were synthesized, and their water sorption, proton transport, and methanol permeation properties were systematically investigated in terms of structural modifications. Carboxylic acid-containing sulfonated polyimides (SPI-Y) were prepared as control materials to be compared with their cross-linked polymers. The carboxylic acid group can be used as a cross-linking site with diols as previously reported.[25]

Figure 2 shows the FT-IR spectrum of protonated SPI-III, consisting of NTDA, SODA, and DBA. The imidization of the SPI-III membrane was confirmed by the characteristic absorption bands for imide such as ν(C═O) in the region of 1680−1710 cm^{-1}, ν(C−N−C) at 1390 cm^{-1} and δ(O═C−N) at 700−740 cm^{-1}. The synthesis of the cross-linked BES−XSPI-III was also confirmed by the corresponding absorption bands. FT-IR absorption bands such as ν(S═O) at 1250 cm^{-1}, ν(SO_3^-) at 1080 cm^{-1} and ν(S−OH) at 918 cm^{-1} indicate the stretching vibrations of the sulfonic acid groups. Finally, a weak absorption band at 1124 cm^{-1} was attributed to the ν(C−O−C) of an ester linkage formed by cross-linking between the polymer chains and BES.

The cross-linking in the BES-cross-linked XSPI membranes was confirmed by the ^{1}H NMR and ^{13}C NMR spectra shown in Figure 3. Similar to the cross-linking reaction using PtG between polymer chains in the previous study,[25] hydroxyl groups (-OH) in the BES react mainly with carboxylic acid groups in the DBA rather than with the sulfonic acid groups in the SODA. Each characteristic peak revealed the formation of a cross-linked carboxylic acid ester in BES−XSPI-III reflecting a relatively high degree of cross-linking in the BES (integral ratio of cross-linked ester to grafted ester (x/g) = 2.34) compared to the PtG (x/g = 1.02) with a similar chain length due to an equilibrium effect.

Solubility. Good solubility in common solvents is a very important factor to consider because the polymer solution is commonly used for making membranes. Generally, polyimides exhibited poor solubility in common organic solvents, and the solubility can be changed with the chemical structure, imidization method (thermal or chemical), and additives. Analogous to common polyimides, the solubility of the SPI membranes was significantly affected by bridging and bulky groups, the

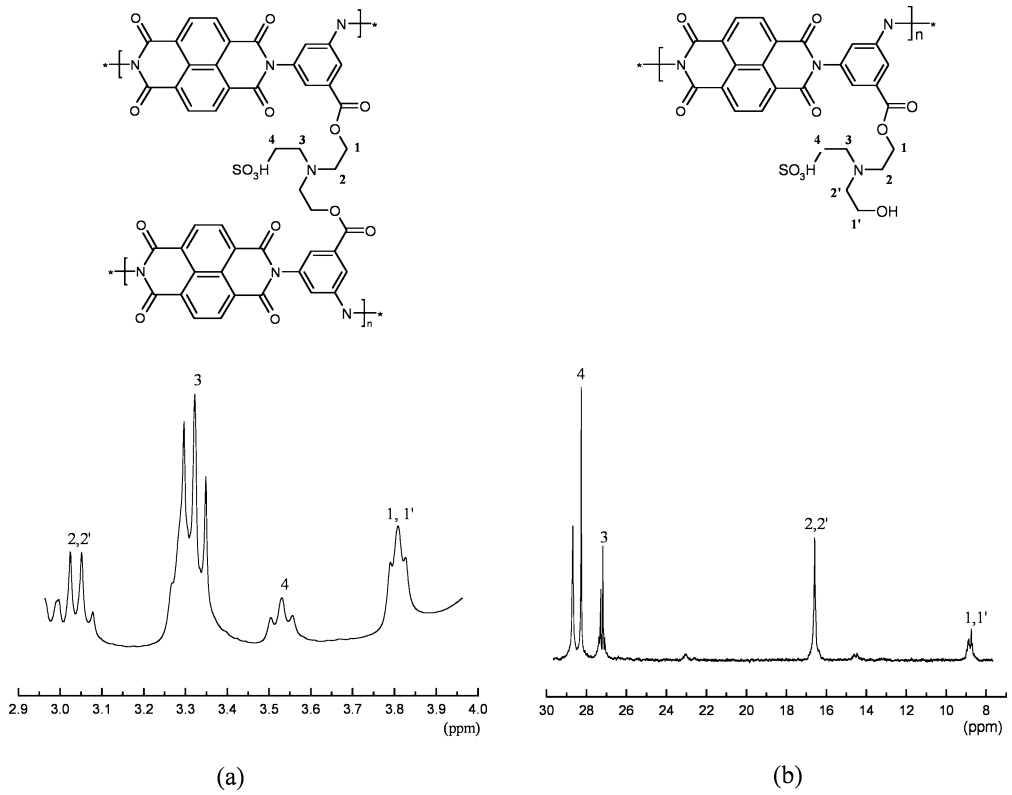

Figure 3. (a) ^{1}H NMR spectrum and (b) ^{13}C NMR spectrum of BES−XSPI-III.

position of substituents, and the sequence of diamine units along the polymer chains.[29,31−33] Here, we used ether-linked SODA and *m*-amino-substituted diamine to achieve better solubility. Typically, the ether (-O-) group between two phenylene rings can make a different intrasegmental configuration to offer better solubility, and *m*-amino-substituted diamine leads to a greater improvement in the solubility than the *p*-amino-substituted diamine, regarding the synthesized polyimide solubility. In the previous study, all SPI membranes in the Et_3N salt form, without cross-linking, were completely soluble in common polar solvents, and after cross-linking with diols, the solubility decreased.[25]

Figure 4a shows the apparent solubility of XSPI membranes cross-linked with PtG and with BES in DMAc and NMP solvents. In both cases, the residual weight of the XSPI membranes in DMAc and NMP solvents increased with the amount of cross-linking agents—PG or BES. Notice that the residual weight of the BES−XSPI membranes was higher than that of the PtG−XSPI membranes, indicating that the solubility of the PtG−XSPI membranes was better than that of the BES−XSPI membranes after cross-linking. In addition, both XSPI membranes were more soluble in DMAc than in NMP.

Figure 4b exhibits the change of the apparent solubility of the BES-cross-linked membranes with varying amounts of BES. As mentioned before, BES reacts preferentially with the carboxylic acid groups in DBA but can also react with the sulfonic acid groups in SODA. Accordingly, the availability of further cross-linking was examined with respect to the solubility in this experiment. Note that the addition of BES in the XSPI resulted in a gradual increase of residual weight, that is, a reduction of solubility, reflecting that further cross-linking was achieved by increasing the amount of BES.

Thermal Stability. The thermal stability of the BES-cross-linked polymer membranes is shown in Figure 5. All BES−XSPI membranes exhibited three distinct degradation steps such as (a) thermal salvation, (b) thermal desulfonation, and (c) thermooxidation of polymer main chains, respectively. The first weight loss began around 100 °C and finished at about 200 °C, which was related to the loss of water molecules bounded in XSPI membranes. The percent of weight loss (mainly water molecules) increased with the amount of sulfonic groups in the XSPI membranes indicating that the water molecules were strongly connected via hydrogen bonding around the sulfonic acid groups. This was consistent with the amount of water uptake in liquid water. The second weight loss from 200 to 400 °C was closely associated with the thermal degradation of the sulfonic acid groups or covalent bonding by cross-linking.[35] The final weight loss above 400 °C represented the thermal decomposition of the main chains or thermooxidation of carboxylic dimers in the side chains.

Water Sorption Behavior. The water content and water state in the sulfonated polymers are very important factors that directly affect proton transport across their membranes. Generally, it is believed that protons can be transported along with hydrogen-bonded ionic channels and cationic mixtures such as H_3O^+, $H_5O_2^+$, and $H_9O_4^+$ in the water medium.[36−38] In a fully hydrated state, sulfonated polymers may dissociate immobile sulfonic acid groups and mobile protons in aqueous solution. Then, the free protons move through a localized ionic network within fully water-swollen sulfonated polymer membranes. Accordingly, the proper water content level should be maintained in sulfonated polymer membranes in order to guarantee high proton conductivity. Simultaneously, the water state such as free water, frozen-bound water, and non-frozen-bound water should be deemed to improve proton conduction across the sulfonated polymer membranes.

Basically, the amount of water uptake in the sulfonated polymers will be strongly dependent upon the amount of sulfonic acid groups and will also be related to IEC values. In non-cross-linked SPI membranes, the increase of weak acid groups

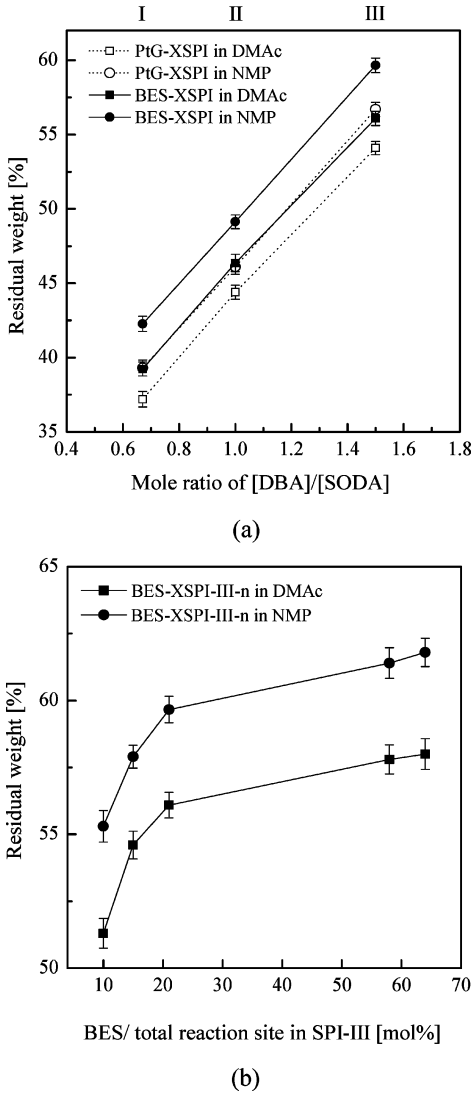

Figure 4. Solubility behavior to polar aprotic solvents of (a) XSPI membranes with different cross-linkers—PtG or BES—and (b) BES−XSPI-III-*n* membranes with various mole percents of BES.

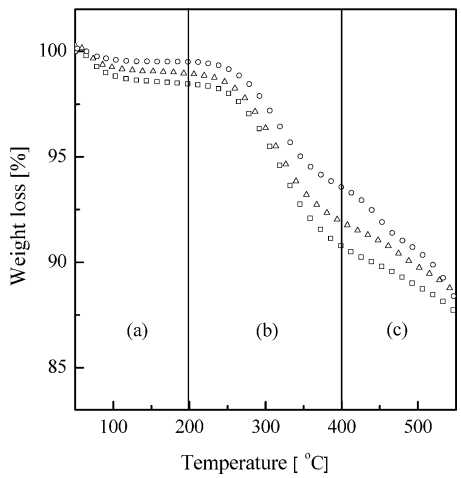

Figure 5. TGA thermodiagram of BES−XSPI membranes under a N_2 atmosphere.

alternative to strong acid groups led to a reduction of the IEC values because the IEC values would be largely affected by a strong acid rather than a weak acid. For PtG-cross-linked SPI (PtG−XSPI) membranes, as expected, the IEC values decreased by increasing the amount of PtG, which is associated with an increase of equivalent weight (EW) as well as a decrease of the sulfonic acid group, as listed in Table 1. On the other hand, the IEC values in the BES-cross-linked SPI (BES−XSPI) membranes were strongly influenced by the sulfonic acid groups of the BES rather than by an increase of the EW due to the addition of BES.

Table 1. Ion Exchange Capacity (IEC) Values Measured Using a Conventional Titration Method and Elemental Analysis Method Compared with Theoretical IEC and the *d*-Spacing Value of the SPI-Y and XSPI-Y Membranes

sample	nominal thickness (μm)	IEC (mequiv g^{-1}) theoretical[a]	titration[b]	EA[c]	*d*-spacing value[d] (Å)
SPI-I	30	2.27	2.20		
SPI-II	25	1.96	1.91		
SPI-III	30	1.90	1.90	1.89	4.21
PtG−XSPI-I	25	2.12	2.09		
PtG−XSPI-II	25	1.82	1.78		
PtG−XSPI-III	30	1.50	1.45		3.86
BES−XSPI-I	30	2.43	2.38	2.32	3.83
BES−XSPI -II	30	2.25	2.17	2.14	3.79
BES−XSPI -III	30	1.98	1.94	1.93	3.75
BES−XSPI-III-10	30	1.76	1.72		3.84
BES−XSPI-III-15	25	1.84	1.80		3.79
BES−XSPI-III-21	25	1.98	1.94		3.75
BES−XSPI-III-58	30	2.38	2.32		3.73
BES−XSPI-III-64	30	2.45	2.38		3.72
Nafion 117	190		0.90[e]		

[a] IEC calculated from the content of sulfonic acid groups per polymer weight. [b] IEC value measured using the back-titration method in ASTM D2187. [c] IEC value measured using elemental analysis (EA). [d] Wide-angle X-ray diffraction (WAXD) patterns recorded at 2θ between 5 and 50° by the reflection scan with nickel-filtered Cu Kα radiation. [e] Measured value.

Figure 6a shows the water uptake behavior of non-cross-linked SPI, BES−XSPI, and PtG−XSPI membranes. In all cases, the water uptake increased with the amount of sulfonic acid groups in the SPI membranes. Note that carboxylic acid groups did not significantly affect the water sorption behavior of the membranes for strong sulfonic acids. The cross-linking of the SPI membranes resulted in a decrease of the water uptake irrespective of the kinds of cross-linking agents. However, in the case of the XSPI-III with the highest mole ratio of [DBA]/[SODA], the cross-linking led to an improvement of the water uptake regardless of the cross-linking between the polymer chains, which implied that the average distance between chains might be broadened by additional cross-linking agent, and consequently the vacant spaces necessary to accommodate more water molecules were formed. Moreover, the introduction of a cross-linking agent with sulfonic acid groups, BES, increased the water sorption capability as compared to the XSPI membranes cross-linked with PtG, which has a similar chain length to BES, but without any ions of fixed charged. Therefore, it turned out that water uptake in sulfonated polymer membranes can be varied by the changes in the microstructure (i.e., hydrophilic channel) as well as by the amount of sulfonic acid.

The effect of the BES content on water uptake behavior of the BES−XSPI-III membranes (at fixed DBA/SODA composition = 6/4) was also observed, as illustrated in Figure 6b. The water uptake increased up to 21 mol % BES content because the amount of sulfonic acid groups had increased with the addition of BES. However, at above a 21 mol % BES content, the water uptake drastically decreased, implying that the effect of cross-linking by BES surpassed that of the sulfonic acid groups in BES. That is to say, the degree of cross-linking drastically increased and then the formation of large water clusters around the sulfonic acid might be excluded. Interestingly, this trend was closely related to the change of the average *d*-spacing value obtained from a WAXD measurement. As a

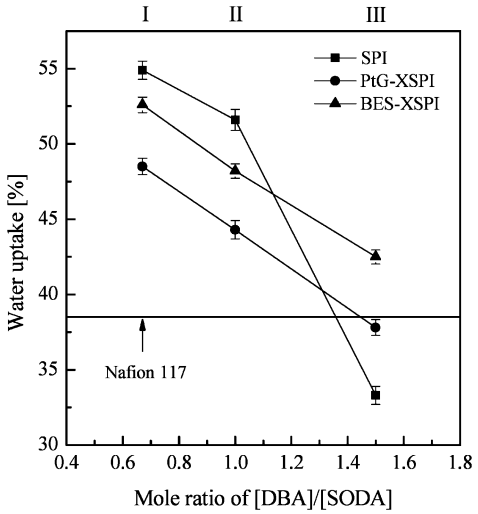

(a)

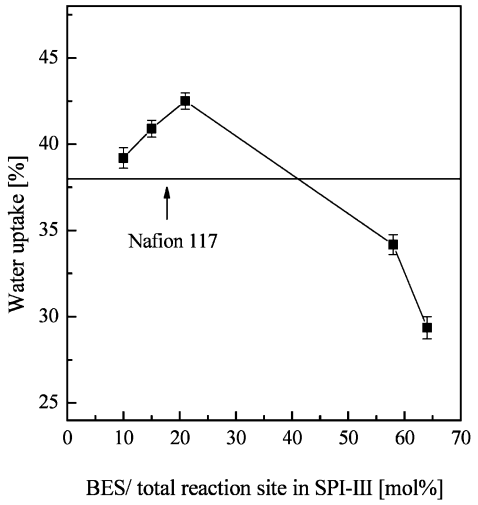

(b)

Figure 6. Water sorption behavior of (a) non-cross-linked SPI and XSPI membranes with different cross-linkers—PtG or BES—and (b) BES−XSPI-III-*n* membranes with different BES content.

result, the free volumes or microvoids to retain water molecules or clusters around negative-charged fixed ions such as sulfonic acids should be precisely controlled to improve proton conduction along with these hydrophilic channels connected with those water channels.

In this study, the water state was also measured using a DSC thermodiagram as shown in Figure 7. In such a DSC curve, a single peak around 0 °C stands for an endothermic peak corresponding to the heat of fusion of free water—the same transition temperature as bulk water. The amount of free water in the SPI and BES−XSPI membranes was obtained from an integration of the endothermic peak area. Then, the amount of bound water was calculated from the difference between the total water and the free water. Table 2 summarizes the amount of free water and bound water. In some cases, bound water can be classified into freezing-bound water and non-freezing-bound water, which is due to a weak or a strong interaction between the water molecules and the polymeric matrix with polar and ionic groups. For non-cross-linked SPI membranes, the decrease of SODA mole ratio in the SPI membranes resulted in relatively a weak water−polymer interaction and then the amount of bound water decreased with total water content. Meanwhile, a completely contrary behavior was discovered in BES-cross-

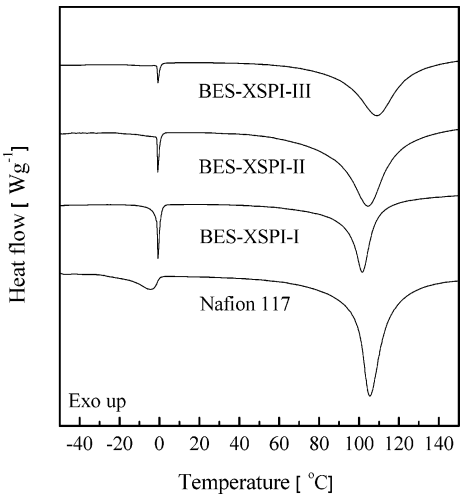

Figure 7. DSC thermodiagram indicating the fusion and vaporization of water in the fully hydrated membranes.

Table 2. Comparison of the State of Water and Activation Energy of the SPI-Y, XSPI-Y, and Nafion 117 Membranes

sample	water content (%)	free water (%)	bound water (%)	ratio [bound]/[total]	activation energy[a] (kcal mol^{-1})
SPI-I	54.9	22.7	32.2	58.7	4.48
SPI-II	51.6	22.5	29.1	56.4	4.37
SPI-III	33.3	15.7	17.6	52.9	4.25
PtG−XSPI-III	37.8	5.5	32.3	85.4	5.33
BES−XSPI-I	52.6	21.1	31.5	59.9	4.54
BES−XSPI-II	48.2	12.3	35.9	74.5	4.69
BES−XSPI-III	42.5	4.9	37.6	88.5	5.58
Nafion 117	38.2	23.5	14.7	38.5	7.32

[a] The activation energy derived from the proton conductivity measurement in the temperature range of 30−90 °C at RH 90%.

linked SPI membranes. The amount of bound water in the BES−XSPI membranes increased with increasing BES content while the amount of free water and total water decreased with the addition of BES. This implied that the bound water can be captured by larger cages around the sulfonic acid groups in the BES than around the sulfonic acid groups located in the main polymer chains. In addition, another endothermic peak at around 100 °C was observed, indicating the heat of vaporization of the water molecules. The increase of the BES content also caused an increase of the vaporization temperature, which indicated stronger water−polymer interactions due to the existence of more bound water content.

Proton Conductivity. The proton conduction through the cross-linked sulfonated polymer membranes will be significantly affected by the water state and water uptake (much related to IEC values or sulfonation level), the cross-linking density, kinds of cross-linkers, and the changes of the microstructure after cross-linking.[14,17−22,25,39] Figure 8a shows the change of proton conductivity of the SPI and PtG− and BES−XSPI membranes as a function of the [DBA]/[SODA] content. Under the same conditions, the conductivities of all sulfonated polyimide membranes were higher than or similar to that of the Nafion 117 membrane (6.6×10^{-2} S/cm). The PtG−XSPI membranes showed a similar conductivity trend to non-cross-linked SPI membranes. On the contrary, the sulfonic acid-containing cross-linker led to a different proton conductivity behavior. As shown in Table 1, the IEC values of the BES−XSPI membranes decreased with the amount of DBA in the SPI, and accordingly a decrease of the proton conductivity was expected because the increase in the amount of sulfonic acid groups by adding BES may not exceed the decrease in the amount of sulfonic acid

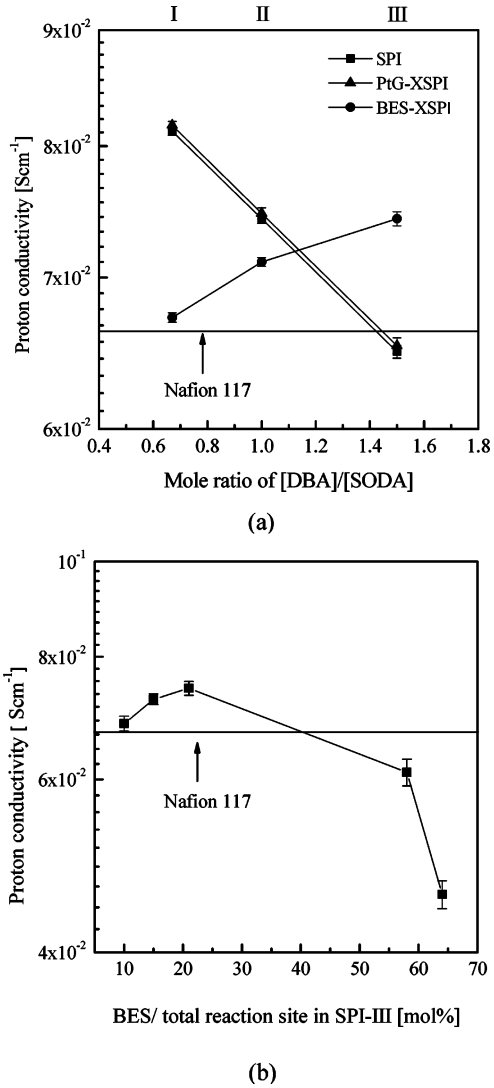

Figure 8. Proton conductivity of (a) non-cross-linked SPI-Y and XSPI membranes and (b) BES−XSPI-III-*n* membranes with various mole percents of BES. (Measurement conditions: 30 °C and 90% RH.)

groups by reducing the SODA content. Actually, the decrease of the IEC values caused a reduction of water uptake as shown in Figure 6a.

Unexpectedly, the proton conductivity of BES−XSPI membranes increased with an increasing [DBA]/[SODA] mole ratio. This might be due to a close contact or connectivity between sulfonic acid groups in XSPI membranes, and also the difference between the acidity of the sulfonic groups in the aromatic groups and that in aliphatic groups. Generally, the acidity of the sulfonic groups attached to the aliphatic chains is stronger than that of the sulfonic groups connected to the aromatic rings.[1,40] In addition, the increase of bound water obtained from the DSC measurement can well explain the proton conductivity behavior in the BES−XSPI membranes. Although the IEC values of the BES−XSPI membranes decreased with BES content in the total composition, increasing the BES content encouraged a strong water−polymer interaction by hydrogen bonding and subsequently led to an increase in bound water content. This large amount of bound water may accelerate the proton transport by the Grötthus hopping mechanism, rather than by the vehicle mechanism. On the basis of the current results that reduced the water uptake but increased the proton conductivity in the BES−XSPI membranes, it can be assumed that the addition of BES in sulfonated polyimides caused denser polymer structures consisting of narrow hydrophilic channels (as seen from the average *d*-spacing data in Table 1) for the protons to conduct effectively through the membranes.

Figure 8b exhibits the change of the proton conductivity of the BES−XSPI membranes depending upon the amount of BES added in a given SPI membrane composition (SPI-III). The proton conductivity of the BES−XSPI membranes increased up to 21 mol % BES content. Above 21 mol % BES, the proton conductivity decreased with additional BES. Apparently, the proton conductivity behavior is very similar to the water uptake trend as shown in Figure 6a. Here, the sulfonic acid-containing chemical cross-linker (BES) played an important role in the proton conductivity in the BES−XSPI membranes, acting as both a cross-linker and a sulfonic acid-supplier. Until 21 mol % BES was reached, the main contribution of the BES would be that of a proton donor rather than a cross-linker. However, above a BES content of 21 mol %, the role of BES would be changed as a good cross-linker to eliminate the microvoids sufficiently such that water clusters are retained around sulfonic acid groups. As a result, the proton conductivity decreased.

The temperature dependence of proton conductivity of the SPI and PtG− and BES−XSPI membranes was obtained using the proton conductivity measurements in a temperature range between 30 and 90 °C. The activation energy for the proton conductivity (E_a) is listed in Table 2. Generally, bound water as a proton transport medium can contribute to the improvement of the proton conductivity at high temperature because a strong interaction between the sulfonated polymer and bound water can retard the quick evaporation of water molecules. Consequently, sulfonated polymers with a high content of bound water have a relatively low dependence of proton conductivity on temperature. The E_a values of all SPI and XSPI membranes were lower than that (7.32 kJ/mol) of the Nafion 117 membrane.

Methanol Permeability. Figure 9 shows the methanol transport behavior of the SPI and XSPI membranes. As depicted in Figure 9a, the change of the methanol permeability was very similar to the results of the IEC values and water uptake behavior. This indicated that methanol transport across the sulfonated polymer membranes was strongly dependent upon the water uptake content, and the methanol permeates through the membranes as complex forms such as $CH_3OH_2^+$ and H_3O^+. The methanol permeability of all SPI and XSPI membranes decreased with increasing DBA content. After cross-linking, irrespective of the type of cross-linking agent, the methanol permeability decreased to nearly 1 order of magnitude lower than that (1.43×10^{-6} cm^2/s) of the Nafion 117 membrane. Interestingly, differing from the results of water uptake and proton conductivity, the BES−XSPI membranes showed the lowest methanol permeability of all the membranes tested in this study. Cross-linking using BES might reduce the vacant spaces that absorb free water molecules and induce a much denser structure to act as a methanol barrier because the existence of the sulfonic acid group in the BES can limit the chain mobility between polymer chains. The reduction of free water in the total water content gradually decreased the methanol permeability.

The effect of the BES content on the methanol permeability is shown in Figure 9b. The change of methanol permeability was similar to that of water uptake and proton conductivity. This indicates that the proton and methanol transport was still strongly related to the change of water uptake by the amount of sulfonation agent and the modification of the cross-linked microstructure. According to the vehicle mechanism, a proton can combine with molecules such as methanol and water and

Table 3. Hydrolytic Stability and Accelerated Peroxide Radical Stability of SPI and XSPI Membranes

	hydrolytic stability[a] (day)	proton conductivity (10^{-2} S cm^{-1})		IEC (mequiv g^{-1})			oxidative stability (h)	
		before	after	before	after	ratio[b] (%)	τ_1 [c]	τ_2 [c]
SPI-I	1.2	8.12	7.79	2.20	2.18	-0.9	23	25
SPI-II	2.3	7.43	7.12	1.91	1.87	-2.1	24	26
SPI-III	3.0	6.49	6.22	1.90	1.86	-2.1	28	31
PtG−XSPI-I	35.4	8.17	7.77	2.09	2.04	-2.4	35	62
PtG−XSPI-II	38.7	7.47	7.12	1.78	1.74	-2.2	36	63
PtG−XSPI-III	42.0	6.53	6.22	1.45	1.42	-2.1	38	65
BES−XSPI-I	12.0	6.72	6.42	2.38	2.32	-2.5	29	45
BES−XSPI-II	13.0	7.11	6.78	2.17	2.15	-0.9	30	48
BES−XSPI-III	14.6	7.43	7.09	1.94	1.90	-2.1	31	50
BES−XSPI-III-10	11.5	6.84	6.50	1.72	1.69	-1.7	27	45
BES−XSPI-III-15	13.2	7.24	6.89	1.80	1.77	-1.7	30	48
BES−XSPI-III-21	14.6	7.43	7.09	1.94	1.91	-1.5	31	50
BES−XSPI-III-58	36.4	6.10	5.82	2.32	2.29	-1.3	34	57
BES−XSPI-III-64	40.9	4.58	4.39	2.38	2.36	-0.8	37	63

[a] The elapsed time that the proton conductivity was not changed within ±5%. [b] The ratio of change in IEC ([(final IEC) − (initial IEC)]/(initial IEC) × 100) at the elapsed time for which the proton conductivity was not changed within ±5%. [c] The elapsed time during that a membrane began to dissolve and dissolved completely in Fenton's reagent, respectively.

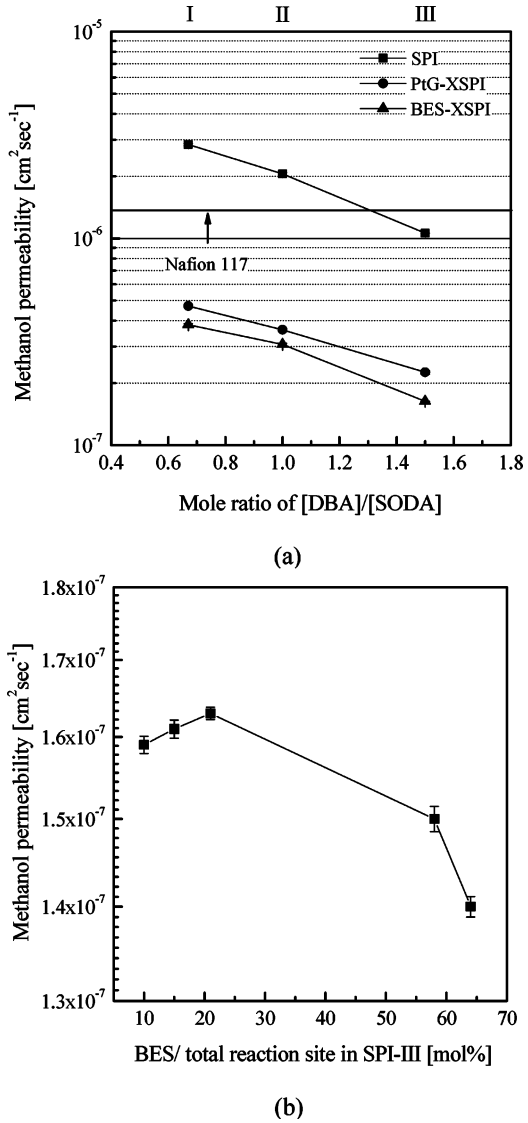

Figure 9. Methanol permeation behavior of (a) SPI-Y and XSPI membranes and (b) BES−XSPI-III-*n* with different BES contents.

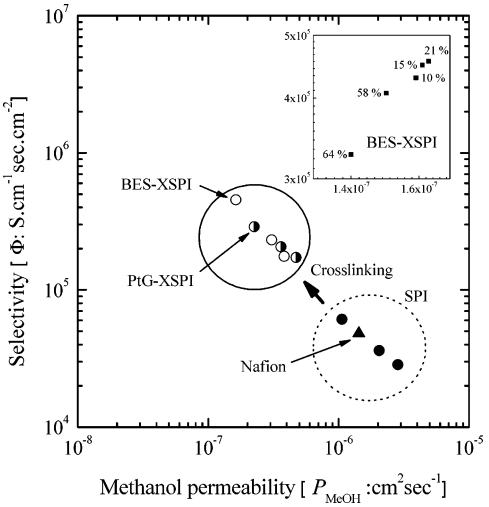

Figure 10. Selectivity ($\Phi = \sigma/P_{MeOH}$) of SPI-Y, XSPI-Y-*n*, and Nafion 117 membranes.

then form a complicated complex such as $CH_3OH_2^+$ and H_3O^+.[41] After that, proton transport can be achieved with the transport of such complex ions. In addition, proton transport can occur between ionic sites such as sulfonic acids in a hopping mechanism. On the other hand, the larger methanol molecule can permeate through relatively huge hydrophilic water channels.

From these results, water sorption, proton transport, and methanol permeation across such sulfonated polymers have very close relationships with each other and hence water/methanol or proton/methanol separation shows a strong tradeoff-type relationship with methanol permeability. Figure 10 shows the selectivity (Φ) or the ratio of proton conductivity (σ) to methanol permeability (P_{MeOH}) of the Nafion 117, SPI, and XPSI membranes. Here, the selectivity means the characteristic factor for evaluating membrane performances considering both the proton conductivity and methanol permeability. Careful attention should be paid in use of the selectivity plot because low methanol permeability and even low proton conductivity give high selectivity. Accordingly, the selectivity must be employed only in comparison with a membrane material with the same order of magnitude in proton conductivity. In this case, the selectivity can be used just as a barometer to develop the best proton-conductive polymer membranes with reduced methanol permeability. The possible values in the current level will be a proton conductivity of above 10^{-2} S/cm and a methanol permeability of below 10^{-6} cm^2 s^{-1} for practical DMFC applications. Nafion 117 and SPI membranes showed very similar proton conductivity and methanol permeability. On the other hand, cross-linked XSPI membranes exhibited about 10 times higher Φ values than the Nafion 117. Among the cross-

linked XSPI membranes, BES−XSPI membranes showed the highest selectivity due to the high proton conductivity and low methanol permeability. The small dotted box in Figure 10 shows that the selectivity was varied with various BES contents, and here the optimal BES content was 21 mol % BES in terms of the selectivity and the proton conductivity.

Membrane Stability. SPI membranes with phthalic imide rings suffer from hydrolytic decomposition in harsh fuel cell conditions.[29,30] Although six-membered naphthalenic polyimides were synthesized to enhance the membrane durability to hydrolysis, it should be further improved for practical fuel cell applications. The hydrolytic stability was investigated by measuring the changes in the proton conductivity and the IEC values after immersion in liquid water at 80 °C and listed in Table 3. Even an aliphatic chemical cross-linker with flexibility led to higher membrane durability to hydrolytic attack in the cross-linked membranes such as PtG−XSPI and BES−XSPI compared with SPI membranes. The hydrolytic stability was dependent on the water uptake and the degree of cross-linking of the SPI membranes. Furthermore, the increase in the BES content from BES−XSPI-I to BES−XSPI-III led to a higher degree of cross-linking and improved membrane durability against hydrolysis. However, the stability in BES−XSPI membranes is still much lower than that in PtG−XSPI membranes due to higher water uptake by the additional sulfonic acid groups in the BES. However, the hydrolytic stability in the BES−XSPI membranes can be improved up to four times by the addition of more BES from 10 to 64 mol % into the same polymer matrix in BES−XSPI-III-*n*. As a result, it was suggested that the proper water content, through the introduction of cross-linkers and the control of cross-linking degree, was necessary to improve the hydrolytic stability as well as the proton conductivity and to reduce the methanol permeability.

The oxidative stability to peroxide radical attack was investigated by measuring the elapsed times that a membrane began to dissolve or when the membrane was broken or lightly bent (τ_1), and a membrane was dissolved completely (τ_2) after immersion of each SPI sample into Fenton's reagent of the 30 wt % H_2O_2 and 0.1 wt % ferrous ammonium sulfate solution at room temperature. Despite the cross-linking by a relatively weak ester bond, all of the cross-linked SPI membranes showed much higher radical stability than the non-cross-linked SPI and other SPIs as reported in Table 3. Though the BES−XSPI membranes showed lower radical stability than the PtG−XSPI membranes without any fixed charged ions, the addition of BES and consequently higher cross-linking degree contributed to the improved free radical stability as well as the hydrolytic stability. In this case, the optimum content of BES is 64% for membrane durability. The cross-linked SPI membranes exhibited higher proton conductivity and lower methanol permeability compared with the Nafion 117 membrane, but their membrane stability did not reach the stringent membrane criteria for practical applications yet. Therefore, we will focus on the development of high-performance-membrane materials with long-term durability under hydrolysis and free radical attacks using the original concept of this study in future work.

Conclusions

Cross-linked XSPI membranes were successfully synthesized via the introduction of a sulfonic acid group containing a chemical cross-linker (BES) into a non-cross-linked sulfonated polyimide containing both a sulfonated diamine and a carboxylated diamine. BES−XSPI membranes in triethylammonium salt form were partially soluble in a polar aprotic solvent, and the content of insoluble residuals increased with increasing BES content. This tendency became more distinct in BES−XSPI membranes containing a higher BES content.

Cross-linking using BES resulted in a higher proton conductivity (up to 1.0×10^{-1} S cm^{-1} at 90 °C and RH 90% with an activation energy of 5.6 kJ mol^{-1}), and lower methanol permeability (1.63×10^{-7} cm^2 s^{-1}) compared with the Nafion 117 (7.39×10^{-2} S cm^{-1} at 80 °C and RH 90% with an activation energy of 7.32 kJ mol^{-1} and 1.43×10^{-7} cm^2 s^{-1}), due to the additional sulfonic acid group in the BES. Although the introduction of BES contributed to improved membrane durability to hydrolysis and peroxide radical attack, the BES−XSPI membranes were still less durable in harsh conditions than PtG−XSPI membranes without any fixed charged ion. The relatively weak membrane stability in BES−XSPI membranes can be improved up to 41 days by adding more BES and consequently increasing the degree of cross-linking.

Despite the fact that the incorporation of BES was effective in improving proton conductivity and decreasing methanol permeability, the addition of BES did not always guarantee the desired enhancement of the proton conductivity and methanol permeability. The content of BES should be optimized in order to obtain the most desirable proton conductivity, methanol permeability, and membrane durability. In this study, the optimum content of BES was 21%, considering only the selectivity and the proton conductivity, while the optimum content of BES was 64% in the methanol permeability and the long-term stability, including the hydrolytic stability and the oxidative stability to peroxide radical attacks.

Acknowledgment. The authors would like to thank the Ministry of Commerce, Industry, and Energy for funding this research (Grant M1042503000704L250300710). C.H.L. is very grateful to the BK 21 Project for a fellowship.

References and Notes

(1) Cram, J. M.; Cram, D. H. *The Essence of Organic Chemistry*; Addison-Wesley: Reading, MA, 1978.
(2) Wei, J.; Stone, C.; Steck, A. E. U.S. Patent 5,422,411, 1995.
(3) Kim, K.; Lee, H. C.; Hong, H. S.; Kim, Y. M. U.S. Patent 2004/0219413 A1, 2004.
(4) Shi, Z.; Holdcroft, S. *Macromolecules* **2004**, *37*, 2084−2089.
(5) Miyatake, K.; Oyaizu, K.; Tsuchida, E.; Hay, A. S. *Macromolecules* **2001**, *34*, 2065−2071.
(6) Nolte, R.; Ledjeff, K.; Mûlhaupt, R. *J. Membr. Sci*. **1993**, *83*, 211−220.
(7) Kerres, J.; Cui, W.; Disson R.; Neubrand, W. *J. Membr. Sci*. **1998**, *139*, 211−225.
(8) Lufrano, F.; Staiti, G. P.; Antonucci, V.; Passalacqua, E. *Solid State Ionics* **2001**, *145*, 47−51.
(9) Karlsson, L. E.; Jannasch, P. *J. Membr. Sci*. **2004**, *230*, 61−70.
(10) Sumner, M. J.; Harrison, W. L.; Weyers, R. M.; Kim, Y. S.; McGrath, J. E.; Riffle, J. S.; Brink, A.; Brink, M. H. *J. Membr. Sci*. **2004**, *239*, 199−211.
(11) Lee, Y. M.; Park, H. B.; Lee, C. H. U.S. Patent 2004/0236038 A1, 2004.
(12) Drioli, E.; Regina, A.; Casciola, M.; Oliveti, A.; Trotta, F.; Massari, T. *J. Membr. Sci.* **2004**, *228*, 139−148.
(13) Wang, F.; Hickner, M.; Kim, Y. S.; Zawodzinski, T. A.; McGrath, J. E. *J. Membr. Sci*, **2002**, *197*, 231−242.
(14) Rhim, J. W.; Park, H. B.; Lee, C. S.; Jun, J. H.; Kim, D. S.; Lee, Y. M. *J. Membr. Sci*. **2004**, *238*, 143−151.
(15) Kaliaguine, S.; Mikhailenko, S. D.; Wang, K. P.; Xing, P.; Robertson, G.; Guiver, M. *Catal. Today* **2003**, *82*, 213−222.
(16) Hickner, M. A.; Ghassemi, H.; Kim, Y. S.; Einsla, B. R.; McGrath, J. E. *Chem. Rev*. **2004**, *104*, 4587−4612.
(17) Xing, P.; Robertson, G. P.; Guiver, M. D.; Mikhailenko, S. D.; Wang, K.; Kaliaguine, S. *J. Membr. Sci.* **2004**, *229*, 95−106.
(18) Mikhailenko, S. D.; Wang, K.; Kaliaguine, S.; Xing, P.; Robertson, G. P.; Guiver, M. D. *J. Membr. Sci.* **2004**, *233*, 93−99.
(19) Guo, Q.; Pintauro, P. N.; Tang, H.; O'Connor, S. *J. Membr. Sci*. **1999**, *154*, 175−181.

(20) Wycisk, R.; Pintauro, P. N.; Wang, W.; O'Connor, S. *J. Appl. Polym. Sci*. **1996**, *59*, 1607−1617.
(21) Graves, R.; Pintauro, P. N. *J. Appl. Polym. Sci*. **1998**, *68*, 827−836.
(22) Kim, D. S.; Park, H. B.; Rhim, J. W.; Lee, Y. M. *J. Membr. Sci*. **2004**, *240*, 37−48.
(23) Hasiotis, C.; Deimede, V.; Kontoyannis, C. *Electrochim. Acta* **2001**, *46*, 2401−2406.
(24) Kerres, J.; Ullrich, A.; Meier, F.; Haring, T. *Solid State Ionics* **1999**, *125*, 243−249.
(25) Park, H. B.; Lee, C. H.; Chung, Y. S.; Lee, Y. M.; Freeman, B. D.; Kim, H. J. *Chem. Mater*., submitted for publication.
(26) Huheey, J. E.; Keiter, E. A.; Keiter, R. L. *Inorganic Chemistry; Principles of Structure and Reactivity*, 4th ed.; HarperCollins: New York, 1993.
(27) Fang, J.; Guo, X.; Harada, S.; Wateri, T.; Tanaka, K.; Kita, H.; Okamoto, K. *Macromolecules* **2002**, *35*, 9022−9028.
(28) Lee, C. H.; Park, H. B.; Lee, Y. M.; Lee, R. D. *Ind. Eng. Chem. Res*. **2005**, *44*, 7617−7626.
(29) Genies, C.; Mercier, R.; Sillion, B.; Petiaud, R.; Cornet, N.; Gebel, G.; Pineri, M. *Polymer* **2001**, *42*, 5097−5105.
(30) Rusanov, A. L. *Adv. Polym. Sci*. **1994**, *111*, 115−175.
(31) Genies, C.; Mericier, R.; Sillion, B.; Cornet, N.; Gebel, G.; Pineri, M. *Polymer* **2001**, *42*, 359−373.
(32) Guo, X.; Fang, J.; Wateri, T.; Tanaka, K.; Kita, H.; Okamoto, K. *Macromolecules* **2002**, *35*, 6707−6713.
(33) Wateri, T.; Fang, J.; Tanaka, K.; Kita, H.; Okamoto, K.; Hirano, T. K. *J. Membr. Sci.* **2004**, *230*, 111−120.
(34) Yin, Y.; Fang, J.; Cui, Y.; Tanaka, K.; Kita, H.; Okamoto, K. *Polymer* **2003**, *44*, 4509−4518.
(35) Kim, D. S.; Park, H. B.; Rhim, J. W.; Lee, Y. M. *Solid State Ionics* **2005**, *176*, 117−126.
(36) Eikerling, M.; Kornyshev, A. A.; Kuznetsov, A. M.; Ulstrup, J.; Walbran, S. *J. Phys. Chem. B* **2001**, *105*, 3646−3662.
(37) Kornshev, A. A.; Kuznetsov, A. M.; Spohr, E.; Ulstrup, J. *J. Phys. Chem. B* **2003**, *107*, 3351−3366.
(38) Spohr, E.; Commer, P.; Kornyshev, A. A. *J. Phys. Chem. B* **2002**, *106*, 10560−10569.
(39) Yen, S. P. S.; Narayanan, S. R.; Halpert, G.; Graham, E.; Yavrouian, A. U.S. Patent 5,795,496, 1998.
(40) Tanabe, K. *Solid Acids and Bases*; Kodansha and Academic Press: Tokyo, New York, and London, 1970.
(41) Won, J. O.; Park, H. H.; Kim, Y. J.; Choi, S. W.; Ha, H. Y.; Oh, I. H.; Kim, H. S.; Kang, Y. S.; Ihn, K. J. *Macromolecules* **2003**, *36*, 3228−3234.

MA052226Y